Characterization of a bis-maleimide triazine resin for multilayer printed circuit boards

by Jeffrey T. Gotro
Bernd K. Appelt

The thermosetting resin investigated in this study was a mixture of bis-maleimide and bis-cyanate, frequently referred to as BT (bis-maleimide triazine). For printed circuit board applications, a brominated epoxy resin was blended with BT to impart flame resistance. Resin curing was extensively investigated using a combination of thermoanalytical techniques (thermal analysis, heated-cell infrared spectroscopy, dynamic mechanical analysis, and microdielectrometry). Differential scanning calorimetry indicated a minimum of two separate reactions. Fourier-transform infrared spectroscopy provided more detailed information on the cross-linking reactions during the curing. The onset of cyclotrimerization was found to appear at 150°C, correlating with one of the peaks observed in the differential scanning calorimetry measurements. Dynamic mechanical methods were used to investigate the viscosity profile during simulated lamination temperature profiles. Microdielectrometry performed simultaneously with parallel-plate rheometry provided further insight into the physical changes that occur during lamination.

Introduction

Traditionally, epoxy-based resins have been used in the fabrication of circuit boards. Increasing circuit densities, higher-power chips, and circuits with increased operating temperatures, along with more stringent insulation resistance requirements, have prompted investigations into alternate materials for board fabrication. Resins of the bis-maleimide triazine (BT) type are a new class of commercially available laminating resins. These resins have substantially better resistance to catastrophic loss of insulation resistance due to conductive anodic filaments that grow along the glass-reinforcing fibers in the laminate [1, 2]. Increased resistance to moisture absorption, excellent chemical resistance, good dimensional stability, low dielectric constant, and low dielectric loss make this type of resin attractive for circuit board applications for which high reliability is critical.

The chemical components and major reaction pathways associated with curing are shown in **Figure 1**. The dominant reactions include the cyclotrimerization of bis-cyanate,

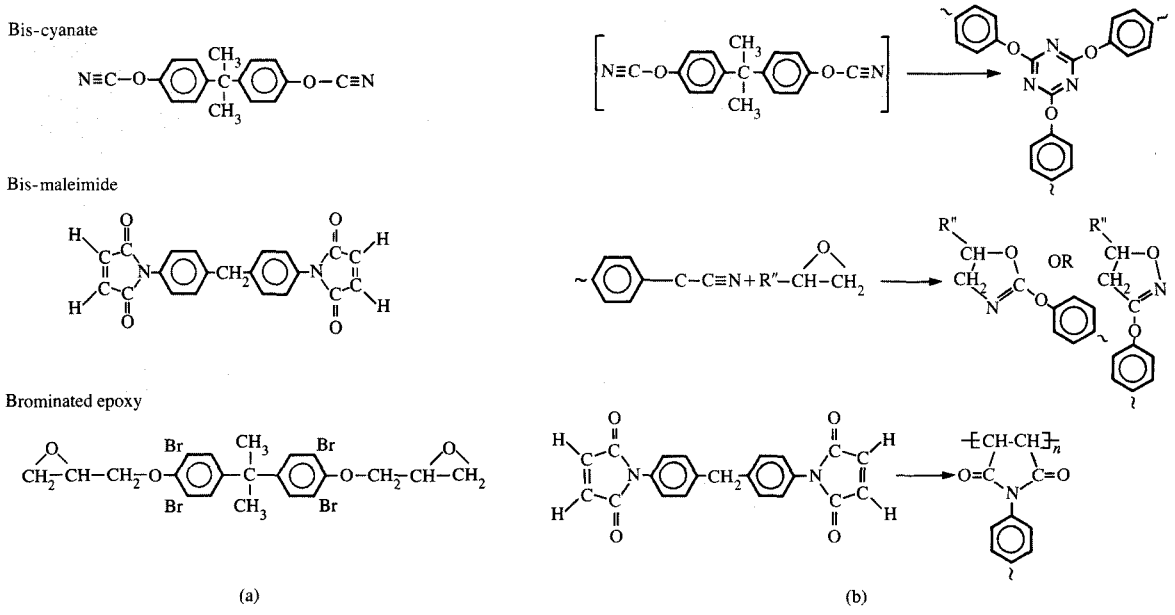

Figure 1

Chemical components (a) and major reaction pathways (b) associated with the curing of a bis-maleimide triazine (BT)/epoxy resin.

reaction of bis-cyanate with epoxides forming oxazoline (or iso-oxazoline) rings, and to a small extent, polymerization of bis-maleimide [3–6]. There are several other possible reactions, but these were either not observed or occur only in a very small percentage compared to the reactions detailed in Figure 1. For circuit board applications, a brominated epoxy resin is included in the formulation to meet flammability requirements [7].

The goal of this study was to investigate the curing characteristics of a BT/epoxy resin formulated for use in printed circuit boards. To accomplish this, resin without glass cloth and resin impregnated onto glass cloth (prepreg) were evaluated using differential scanning calorimetry (DSC), heated-sample-cell Fourier-transform infrared spectroscopy (FT–IR), oscillatory parallel-plate rheometry, and microdielectrometry.

Experimental methods

The BT resin was supplied by the Mitsubishi Gas Chemical Company, and the catalyst was zinc octanoate, as recommended by Mitsubishi [7]. A brominated diglycidyl ether of bis-phenol A (DGEBA) was added to impart flame resistance. The data presented in this work are based on a formulation containing 70% BT and 30% epoxy. The concentrations of the resins, their molecular weight, and their molecular weight distributions can be varied to achieve the desired final laminate properties.

Differential scanning calorimetry (DSC) was performed using a Perkin-Elmer DSC-2 calorimeter with a data station. The heating rate was maintained at 20°C/min, scanning from 0°C to 340°C. The sample size was between 5 and 10 mg. Heats of reaction were calculated from the area under the exotherm. The glass-transition temperature T_g was recorded as the onset of the endothermic baseline deflection. The ultimate T_g (T_g of the fully cured resin) was determined after samples were cured at 250°C for one hour. In the case of prepregs, the resin was flaked off the cloth prior to analysis. The total heat of the reaction was measured from vacuum-dried varnish and was used as the reference in computing the percent conversion.

Fourier-transform infrared spectroscopy (FT–IR) was performed using an IBM Instruments Model IR/85 FT–IR equipped with a temperature-controlled sample cell (Accuspec Corporation). Thin films of the resin on sodium chloride crystals were prepared by solvent-casting methods. The temperature of the samples was increased by 10°C/min to the desired reaction temperatures (150, 175, and 200°C), and then maintained isothermally (total heating time was 60 minutes). The FT-IR spectra were obtained at 90-second intervals. Peak areas were normalized using an internal standard (820 cm^{-1}, corresponding to the in-phase, out-of-plane aromatic hydrogen wagging vibration).

Prepregs were prepared by impregnating woven glass fabric with a resin solution using standard solvent-

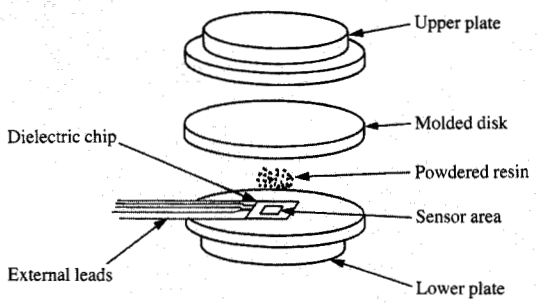

Figure 2

Exploded view of the parallel plates, dielectric sensor, molded resin disk, and placement of powdered resin used for simultaneous dielectric and dynamic mechanical analysis.

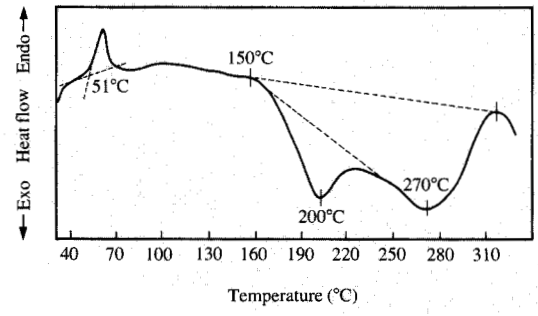

Figure 3

Typical DSC thermogram of a BT/epoxy prepreg. From [13], reproduced with permission.

impregnation methods. Samples for dynamic mechanical analysis were prepared by shaking the resin off the cloth, removing stray glass fibers, and molding the powdered resin into 2.54-cm-diameter disks approximately 0.15 cm thick. Void-free sample disks could be obtained without advancing the resin.

Dynamic mechanical analysis was performed using a Rheometrics System Four rheometer in the dynamic parallel-plate geometry. A sinusoidally varying strain (at a frequency of 1 Hz and a strain amplitude of 2.0%) was applied to the sample. A strain gauge transducer was used to measure the resulting stress amplitude and phase angle, from which the dynamic moduli and viscosity were obtained [8]. The heating rates were varied from 3 to 20°C/min. Samples were scanned from 30 to 175°C and were held at 175°C for specified times. The sample temperature was monitored with two thermocouples embedded in the lower plate, in contact with the resin sample.

A Micromet Eumetric System II microdielectrometer was used for dielectric analysis. The system used for that purpose has been described in detail elsewhere [9–12]. The electrode configuration was an interdigitated comb pattern. The sensor package consisted of the electrode, bond pad area, transistors, thermal diode, and encapsulated lead wires. The dielectrometer can be used in a frequency range of 0.005–10000 Hz. The cure-analysis experiments were conducted at 100 Hz, chosen arbitrarily since it produced a full-scale signal at all heating rates.

Aluminum disposable plates were used for the parallel-plate analysis. The dielectric sensor was fitted tightly in a milled notch in the center of the bottom plate, permitting alignment of the top of the sensor with the surface of the bottom plate. A small amount of powdered resin was placed over the electrode area and the resin disk was inserted between the parallel plates.

A schematic of the parallel plates, resin disk, and the dielectric sensor arrangement is shown in **Figure 2**. The prepreg softened during the initial heating and flowed into the comb electrodes, ensuring complete electrode contact. Good contact was confirmed by cross-sectioning selected sensors after the run was completed. In order to obtain dielectric information early in the heating cycle, a small amount of resin powder was placed over the electrode area and the sensor was placed on a hot plate heated to 90°C. This allowed the resin to flow and completely cover the electrode pattern. After the resin softened, the sensor was removed from the hot plate and quickly cooled. Care was taken to minimize the length of time the resin was exposed to heat. DSC analysis before and after sample preparation verified that this procedure did not advance the resin.

Results and discussion

The thermogram of BT/epoxy prepreg shown in **Figure 3** exhibited two distinct yet overlapping peaks. The combined heat of reaction was determined to be 60 cal/g. To a first-order approximation, the first peak (T_{max} = 200°C) contained 10 cal/g, and the second (T_{max} = 270°C) contained 50 cal/g. The shape of the exotherm suggested multiple reactions, with complete and rapid reaction expected only when the temperature is close to the second T_{max} (effects of conversion on T_g are discussed below).

To assess the dependence on temperature during prepreg curing, isothermal DSC experiments were conducted at 175, 200, 225, and 250°C. In **Figure 4**, the residual heat of reaction was plotted versus time for the isothermal experiments. The residual heat of reaction decreased rapidly to a plateau value for each of the temperatures except 250°C. Even prolonged exposures at the lower temperatures (for

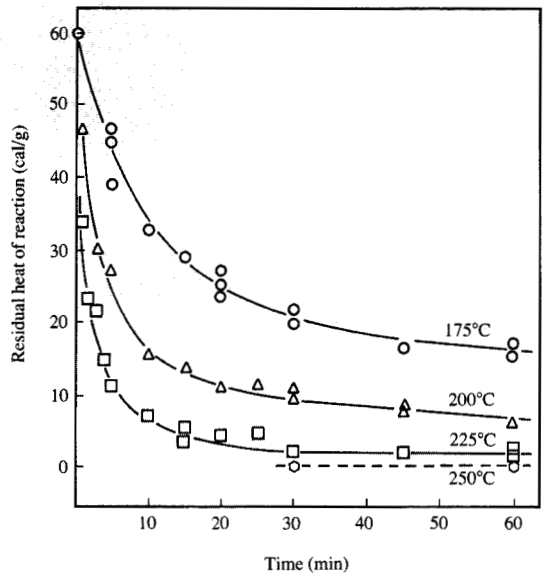

Figure 4

Residual heat of reaction versus time for several reaction temperatures. From [13], reproduced with permission.

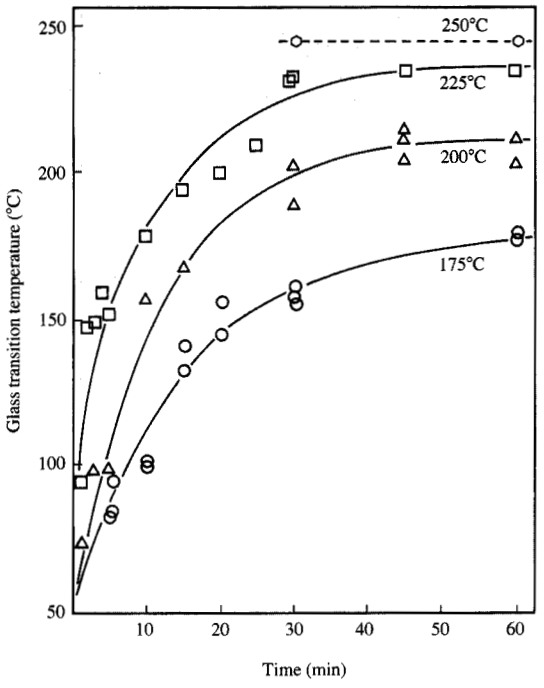

Figure 5

Glass transition temperature versus time for several reaction temperatures. From [13], reproduced with permission.

more than two hours) did not lead to complete reaction, but to a conversion which was a function of the curing temperature. Thus, a metastable state was attained that was subject to change only if the sample was exposed to the same or higher temperatures for an extended period of time. The relative rates of reaction at 175, 200, and 225°C were deduced from the residual heats of reaction. The activation energy for the combined thermal reactions was estimated to be 25 kcal/mole.

The glass-transition temperature at high conversion appeared to be a much more sensitive way to monitor the extent of curing [14, 15]. Initially, T_g rose rapidly until the reaction temperature was reached (see **Figure 5**). Above the reaction temperature, T_g increased slowly and approached a level about 20–30°C above the cure temperature. Only when the resin was cured at 250°C could a fully cured system be obtained, with a T_g of about 240°C. These observations were in agreement with the Time Temperature Transformation concept of Gillham and Enns [16, 17]. Complete reaction in a reasonable period of time can only be achieved if the reaction temperature exceeds or is equal to the ultimate T_g of the system.

For a system of this complexity, the terms "conversion" and "rate of reaction" have limited utility, since calorimetry observes the thermal events of all chemical reactions. Also, 100% conversion (or ultimate conversion) is used here in the context of consuming all of the reactive functionalities within the described experiment. Thermosets build networks which can lead to entrapped or hindered functionalities which may prevent full (or 100%) conversion, in the strict sense of the definition. In the case of the BT/epoxy resin studied here, there appear to be several distinct reactions occurring during curing. For these reasons an experimental method was developed to examine the individual reactions using a heated sample cell in the FT-IR.

The curing reactions were characterized using the epoxy ring vibration (915 cm^{-1}), the aromatic cyanate vibration (-C≡N, 2270 cm^{-1}), and the triazine ring vibration (-C=N-, 1560 cm^{-1}).

The lamination process used to fabricate multilayer circuit boards involves nonisothermal curing. In order to simulate various lamination conditions, the BT/epoxy samples were heated from 30 to 150°C, 30 to 175°C, and 30 to 200°C at a rate of 10°C/min. After reaching the upper temperature, the cell was maintained at that temperature until the end of the data acquisition time (total time was 60 minutes). Obviously, isothermal curing studies allow more precise determination of the reaction kinetics, but due to the complicated

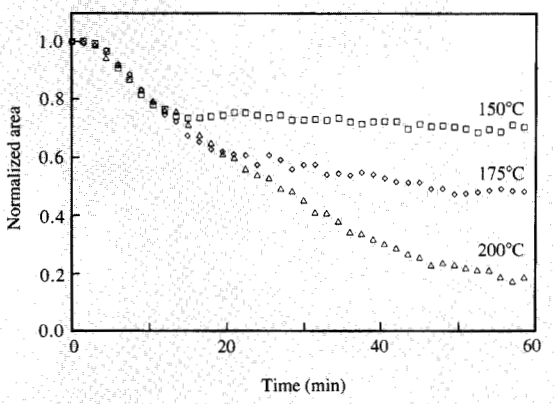

Figure 6

Normalized epoxide vibration versus time. Temperatures were increased at 10°C/min until the indicated levels were reached, and then maintained at those levels. From [13], reproduced with permission.

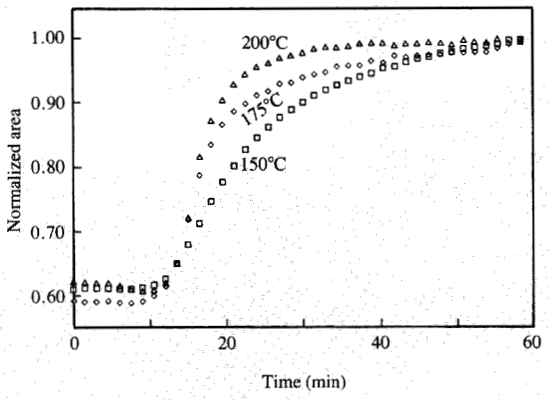

Figure 8

Normalized triazine ring vibration versus time. Temperatures were increased at 10°C/min until the indicated levels were reached, and then maintained at those levels. From [13], reproduced with permission.

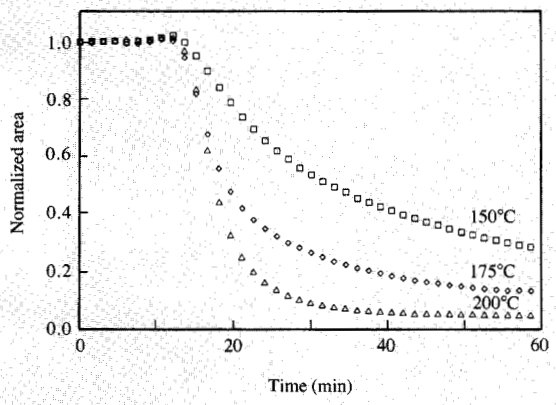

Figure 7

Normalized aromatic cyanate vibration versus time. Temperatures were increased at 10°C/min until the indicated levels were reached, and then maintained at those levels. From [13], reproduced with permission.

chemistry, the main thrust of this work was to monitor the major reactions during temperature profiles which were similar to those used during typical board fabrication.

In **Figure 6**, the normalized epoxide vibration is plotted versus time for the three cases. As can be seen, because use was made of the same initial heating rate, the initial epoxide reaction rates followed the same curve. The epoxide reaction begins at about 70°C; the extent of reaction is a function of the final temperature. When the final temperature is 150°C, the reaction appears to "freeze in" at a level of about 30% in reacted epoxy. For reactions at 175°C, the epoxy continues to react for a limited time before reaching a conversion of 55%. Only at 200°C does the epoxy continue to react extensively, approaching a level of 85% in conversion of epoxy functionalities. The conversion might possibly have been higher, but the experiment was terminated after 60 minutes.

Figures 7 and **8** show the normalized cyanate and triazine vibrations, respectively. The rapid decrease of the cyanate vibration begins at about 150°C, with the reaction rate and ultimate conversion a strong function of the reaction temperature. Only at 200°C did the consumption of cyanate appear to level off.

To compare the relative reaction rates, the rate of cyanate consumption (–C≡N decrease) and the rate of triazine formation (–C=N– increase) were investigated. From the data in Figures 7 and 8, the maximum reaction rates were determined by plotting the incremental slope as a function of time for each of the temperature profiles. At 150°C, the ratio of the rate of cyanate consumed to the rate of triazine double-bond formation was 1:1. At 175°C, the ratio of the rate of cyanate consumed to the rate of triazine formed was 1.2:1, and at 200°C, this ratio was 1.5:1. The cyanate/triazine data indicated that at 150°C, cyclotrimerization was the

predominant reaction pathway. The epoxy data indicated that about 30% of the epoxy groups were consumed at 150°C. This suggests that an interpenetrating network of epoxy–epoxy and triazine rings were formed at the 150°C reaction temperature. As the final reaction temperature increased, the consumption of cyanate exceeded the rate of trimerization, indicating that the cyanate group was participating in additional reactions, most likely the formation of oxazoline ring structures [Figure 1(b)].

The FT-IR data indicated that the DSC peak centered at 200°C was primarily due to the cyclotrimerization reaction, although there clearly appeared to be cyanate–epoxy reactions occurring in this temperature range. The extent of cyanate conversion was a strong function of the reaction temperature. The amount of unreacted cyanate was 28% at 150°C, 14% at 177°C, and 5% at 200°C. Ultimate conversion appeared to be reached only above 200°C, with continued reaction proceeding very slowly at lower temperatures.

In summary, infrared data indicated that at temperatures between 70 and 150°C, 30% of the epoxy groups reacted slowly, and the cyanate reaction started at 150°C. This temperature corresponded to the initial exothermic baseline deflection in the prepreg DSC trace (Figure 3). The exothermic peak with $T_{max} = 200$°C could be partially attributed to the cyclotrimerization reaction. Above 150°C there were competing reactions in epoxy–cyanate products, triazine ring structures, and epoxy–epoxy homopolymerization. The triazine ring formation appeared to be complete at 175 and 200°C, with residual cyanate functionality detected at both of these temperatures. From the data presented here, the exact chemical mechanisms accounting for the high-temperature (270°C) peak in the DSC could not be determined. From the FT-IR data, there was very little cyanate or epoxy functionality remaining after reaction at 200°C. Nevertheless, the DSC peak at 270°C is fairly large. A fraction of this peak may be due to remaining epoxy–cyanate and epoxy–epoxy reactions, but the majority of this peak appears to be due to the polymerization of bis-maleimide.

Lamination of a B-staged thermosetting resin is a critical step in the fabrication of multilayer printed circuit boards. During lamination the resin undergoes major physical changes. As the temperature increases, the prepreg (B-staged resin) softens, becomes a fairly low-viscosity liquid, and subsequently cross-links to form a gel. Further chemical reactions during the lamination process develop a thermoset network with a high glass-transition temperature.

Extensive work has been performed to investigate the various factors influencing curing and flow during lamination [18, 19]. To investigate the physical changes occurring during curing, microdielectrometry and dynamic oscillatory parallel-plate rheometry methods were used.

In the case of cure monitoring of thermosetting polymers, the most useful information is obtained by use of

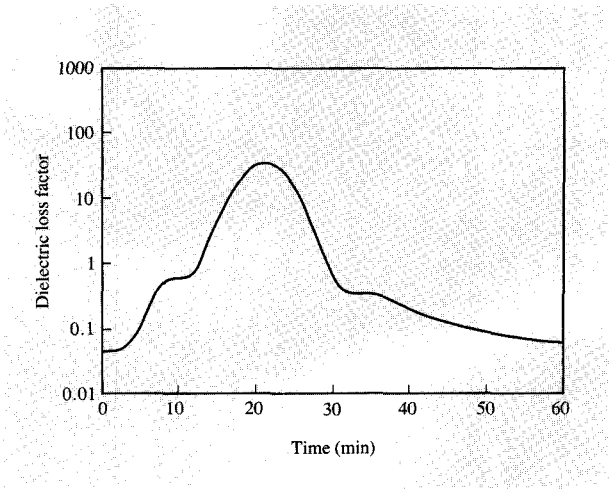

Figure 9

Dielectric loss factor at 100 Hz as a function of time for BT/epoxy resin heated at 5.8°C/min to a temperature of 175°C and maintained at that temperature. Frequency was 100 Hz.

microdielectrometry, specifically by examining the dielectric loss factor. The latter comprises two components, one due to dipole orientation with the applied field and the other arising from bulk (or ionic) conduction. A simple relationship for the loss factor may be written

$$\epsilon'' = \sigma/\omega\epsilon_0 + \epsilon''_d,$$

where ϵ'' is the dielectric loss factor, σ is ionic conductivity, ϵ_0 is the permittivity of vacuum (8.85×10^{-14} F/cm), ω is the frequency, and ϵ''_d is the sum of all dipolar contributions. The last depends on the distribution of dipole relaxation times for the given polymer. For the purposes of this discussion, an exact formulation of the dipolar contribution is not necessary. For further details, the reader is referred to an excellent review by Senturia and Sheppard [9]. In summary, the loss factor is composed of two contributions, the first resulting from frequency-independent ionic conduction, and the second from frequency-dependent dipole orientation [9, 10].

For a thermosetting polymer, at temperatures in the vicinity of T_g, contributions from dipole relaxation mechanisms dominate the signal. As the temperature increases, the contribution from ionic conduction becomes significant. The ionic conduction mechanism is mostly attributed to residual ionic species formed during monomer synthesis [20, 21]. For commercial epoxy resins, the residual ion concentration is typically of the order of tens of ppm [22]. These residual impurities actually provide a very useful probe of the resin system. For a given resin system, the ion concentration and ionic charge are constant, and as a result, the conductivity is proportional to the ionic mobility. The

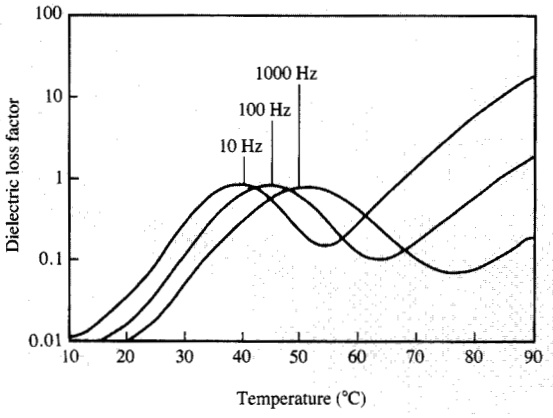

Figure 10

Dielectric loss factor as a function of temperature at various frequencies for BT prepreg heated at 2°C/min.

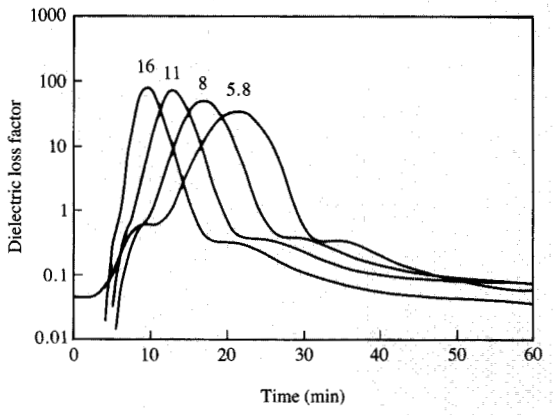

Figure 11

Dielectric loss factor at 100 Hz as a function of time at various heating rates (in °C/min). Frequency was 100 Hz.

ionic mobility is a direct function of the polymer segmental mobility, which changes dramatically as the resin liquifies, vitrifies, or cross-links. Thus, the ionic conductivity (or loss factor) is very useful for monitoring curing. In light of this, the BT/epoxy resin studied here was examined in the microdielectrometer without purification.

A typical lamination process involves heating the B-staged prepreg at a given heating rate from room temperature to the curing temperature, usually in the range of 160–180°C. The dielectric loss factor which was obtained for a BT prepreg under similar conditions is plotted as a function of time in **Figure 9**. The prepreg was heated at 5.8°C/min to 175°C and maintained at that temperature; the powdered resin was first heated and allowed to flow into the comb electrode.

Therefore, dielectric data were obtained over the entire cure cycle. As the resin was heated, the chain-segmental mobility increased with temperature, causing an increase in the loss factor. The first feature observed was the peak occurring after 60°C (10 min). This peak was frequency-dependent and corresponded to dipolar contributions to the loss factor. The frequency dependence was verified by scanning several frequencies during the heating. The frequency dependence can be seen in **Figure 10**, where the dielectric loss factor is plotted as a function of temperature at 10, 100, and 1000 Hz.

The frequency-dependent peak can be accounted for by the increased mobility of polar chain segments at higher temperatures. In the low-temperature regions, the motion of chain segments is too sluggish to follow the alternating field. At intermediate temperatures, the chain-segmental mobility increases. Polar groups begin to move in response to the applied electric field, but their motions lag behind the field, causing a continuous loss of energy. The loss of energy goes through a maximum and then decreases as molecular motion becomes less and less restricted, allowing more alignment with the applied field.

At increased temperatures, the dielectric loss factor takes a dramatic upturn, corresponding to the onset of ionic conductivity. The ions are small compared to the size of the polymer chains in a complex network. Thus, ionic conductivity depends on the small-scale segmental mobility. As the temperature continues to increase, chain-segmental mobility increases, leading to an increase in the ionic conductivity. Subsequently, the cross-linking reaction causes the molecular weight and degree of branching to increase rapidly. This begins to restrict chain-segmental mobility and thus also ionic conduction. The frequency-independent maximum in the loss factor occurs when the chain-segmental mobility has decreased to the state at which the ionic conductivity is reduced. As the cross-linking reaction proceeds, tightening of the network leads to a decrease in the ionic contribution to the loss factor.

As the network mobility decreases, the loss factor due to ionic conductivity should follow. With chemical conversion, the resin should vitrify (transition from rubbery to glassy state), increasing the T_g to above the curing temperature. Associated frequency-dependent dipole peaks are expected (shoulder after maximum).

In **Figure 11** the dielectric loss factor at 100 Hz is plotted as a function of time for various heating rates. The 5.8°C/min data were previously shown in Figure 9. The other data were obtained using powdered resin covering the sensor; thus data were not available until the resin softened

and covered the electrodes. As can be seen, the time required for the occurrence of the loss factor maximum decreased with increasing heating rate.

The viscosity was measured for each of the temperature profiles used to obtain the data shown in Figure 11. The complex viscosity at these and several additional heating rates is plotted as a function of time in **Figure 12**. As the temperature increases, the resin softens at the T_g of the prepreg. With continued heating, the viscosity decreases. When the chemical kinetics of the cross-linking reactions are faster than the decrease in the viscosity due to heating, the viscosity reaches a minimum and subsequently increases. As the chemical reactions continue, the molecular weight and cross-link density increase, causing the viscosity to increase. The heating-rate dependence of the minimum viscosity follows the same trend observed in the loss-factor maximum. From the fastest to the slowest heating rates, the minimum viscosity changes by about half an order of magnitude.

To obtain a direct correlation of the dielectric events to physical changes in the resin during the curing cycle, simultaneous dynamic dielectric and dynamic mechanical analyses were carried out. **Figure 13** shows the change with time of the complex viscosity and the dielectric loss factor when the temperature was increased at the 5.8°C/min heating rate to 175°C and then maintained at that level. A frequency-dependent dipole peak was found to occur at the point where the resin softens and the viscosity decreases rapidly. As the resin softens, the ionic conductivity begins to dominate the loss factor. The viscosity then reaches the minimum value and begins to increase due to decreased segmental mobility as more cross-links are formed. Further cross-linking causes a decrease in the ionic conductivity. The resin continues to react at the isothermal temperature until vitrification occurs, resulting in the appearance of a frequency-dependent dipole peak such as that seen in the figure.

The vitrification event was clearly evident in the behavior of the viscosity: At vitrification the viscosity took a rapid upturn and increased considerably. The rheometer oven was maintained at a constant temperature and dielectric data acquisition continued for about 55 minutes. The diffuse shoulder on the dielectric loss factor peak at long times occurred at approximately the same time as the rapid upturn in the viscosity. The appearance of dipole peaks during isothermal curing at temperatures below the ultimate T_g has been observed by several authors [9, 10, 23].

As can be seen, the minimum in the viscosity and the maximum in the dielectric loss factor did not occur at the same time. The indicated difference of about two minutes may have been due to a temperature gradient across the plate. During heating, because of radial symmetry, the temperature at the center of the plate was expected to be lower than at its edges; thus the dielectric response was measured on the coolest part of the sample. The viscosity measurement was most dependent on the temperature of the warmest resin, since the outer edge of the plate is expected to have more of an influence on the torque. Thus, the observed time difference was not considered to be unreasonable.

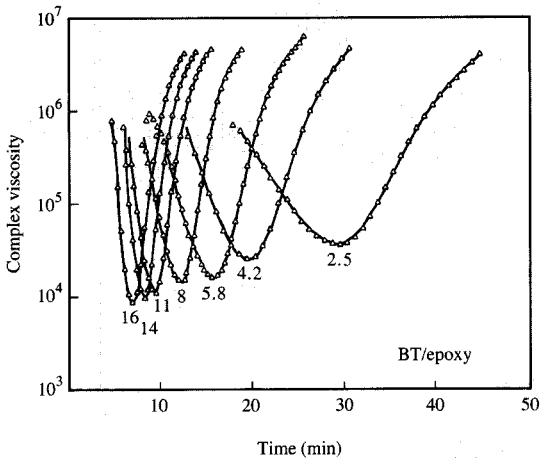

Figure 12

Complex viscosity as a function of time for various heating rates (in °C/min).

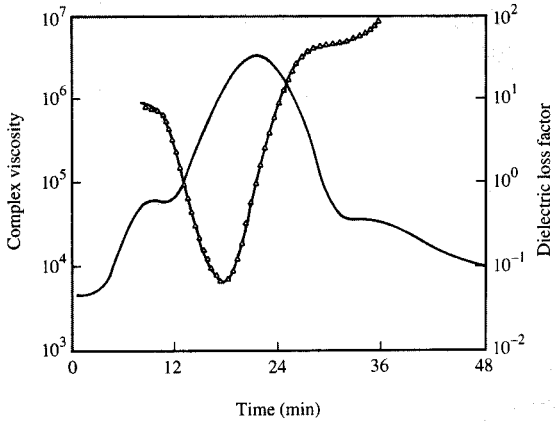

Figure 13

Complex viscosity (Δ curve) and dielectric loss factor (solid curve) at 100 Hz (measured simultaneously) plotted as a function of time. Temperature was increased at 5.8°C/min to a temperature of 175°C, and then maintained at that level.

Conclusions

Isothermal differential scanning calorimetry studies have indicated that the residual heat of reaction decreases rapidly to a plateau level for each of the reaction temperatures which were used, except 250°C, where the reaction goes to completion. Prolonged exposures at reaction temperatures below 250°C did not lead to complete reaction. Thus, a metastable state is attained which only changes if the sample is exposed to an elevated temperature. From the differential scanning calorimetry studies, it appears that T_g can reach a value of 20–30°C above the reaction temperature.

Insight into specific reactions during curing was obtained from heated-cell Fourier-transform infrared spectroscopy experiments. The cyclotrimerization reaction started at 150°C; the reaction rate increased with temperature, and the amount of triazine formed was independent of reaction temperature. Thirty percent of the epoxy groups reacted between 70 and 150°C, with ultimate conversion of the epoxide functionality being a strong function of temperature. The amount of unreacted cyanate was found to be temperature-dependent, with an ultimate level of conversion being reached only above 200°C. At lower temperatures there was a slower but continued reaction. Above 150°C the reaction scheme is quite complex, with the formation of epoxy–cyanate products, cyclotrimerization of cyanate forming triazine ring structures, and epoxy–epoxy homopolymerization. Polymerization of bis-maleimide is also a possible reaction, but it was not investigated in this study. The chemistry of the BT/epoxy system is very complex; further work will be necessary to fully understand its curing mechanisms.

Curing was monitored using microdielectrometry and dynamic mechanical analysis. The small sensor of a microdielectrometer was embedded in its lower plate during oscillatory parallel-plate rheometry. This allowed simultaneous measurement of the dielectric and dynamic mechanical properties. It was found that a frequency-dependent dipole relaxation during heating occurred at the onset of vitrification. The frequency-independent ionic conductivity peak appeared to track with segmental mobility (viscosity). A frequency-dependent dipole relaxation which appeared at elevated temperatures corresponded to vitrification. Microdielectrometry was found to be a useful method of monitoring the curing of high-performance thermosetting polymers. Additional work is in progress to develop and investigate curing models using rheological and dielectric data.

Acknowledgments

The authors would like to thank G. Kohut (FT-IR) and J. Wernke (DSC) for their assistance in acquiring experimental data. M. Yandrasits performed the dielectric experiments and was extremely helpful in developing the simultaneous rheology–dielectric method.

References

1. T. L. Welsher, J. P. Mitchell, and D. J. Lamdo, *Proceedings, 18th Annual IEEE Conference on Reliability Physics*, Las Vegas, April 1980.
2. S. Moteori, H. Kimbara, M. Gaku, and S. Ayano, *Electrical and Electronics Insulation Conf. Proc.* **15**, 168 (1981).
3. M. Gaku, K. Suzuki, and N. Ikeguchi, *Proceedings, 13th IEEE Electrical and Electronics Insulation Conference*, Chicago, September 1977.
4. S. Ayano, *Chem. Econ.* **25**, 12 (1978).
5. S. Ayano, *Chem. Econ. & Eng. Rev.* **10**, 25 (1977).
6. *Nikkei Electronics*, No. 184, 40 (1978).
7. Product Bulletin, Fourth Edition, Bismaleimide–Triazine Resin, Mitsubishi Gas Chemical Company, Tokyo, 1984.
8. J. Ferry, *Viscoelastic Properties of Polymers*, 3rd Ed., John Wiley & Sons, Inc., New York, 1982.
9. S. Senturia and N. Sheppard, *Adv. Polym. Sci.* **80**, 1 (1986).
10. N. Sheppard, Ph.D. Thesis, Massachusetts Institute of Technology, Cambridge, MA, 1986.
11. S. Senturia and S. Garverick, U.S. Patent 4,423,371, 1983.
12. S. Senturia, N. Sheppard, H. Lee, and D. Day, *J. Adhes.* **15**, 69 (1982).
13. J. Gotro, B. Appelt, and K. Papathomas, *Polym. Compos.* **8**, 39 (1987).
14. B. K. Appelt and P. J. Cook, in *Analytical Calorimetry*, Volume 5, J. F. Johnson and P. S. Gill, Eds., Plenum Publishing Co., New York, 1984, p. 57.
15. A. Hale, C. Macosko, and H. Bair, *Society of Plastics Engineers, Technical Papers, ANTEC 87*, Los Angeles, 1987, Vol. 33, p. 1116.
16. J. K. Gillham, in *Developments in Polymer Characterization, Part 3*, J. V. Dawkins, Ed., Applied Science, London, 1982.
17. J. B. Enns and J. K. Gillham, *J. Appl. Polym. Sci.* **28**, 2567 (1983).
18. B. Appelt, J. Gotro, G. Schmitt, T. Ellis, and J. Wiley, *Polym. Compos.* **7**, 91 (1986).
19. J. Gotro, B. Appelt, and T. Ellis, *Society of Plastics Engineers, Technical Papers, ANTEC 86*, Boston, 1986, Vol. 32, p. 371.
20. R. Fava and A. Horsfield, *Brit. J. Appl. Phys. (J. Phys. D)* **1**, 117 (1968).
21. H. Lee and K. Neville, *Handbook of Epoxy Resins*, McGraw-Hill Book Co., Inc., New York, 1967.
22. W. W. Wright, *Brit. Polym. J.* **15**, 224 (1983).
23. M. Olyphant, *Proceedings, Sixth IEEE Electrical Insulation Conference*, 1965, p. 12.

Received November 10, 1987; accepted for publication April 8, 1988

Jeffrey T. Gotro *IBM Systems Technology Division, 1701 North St., Endicott, New York 13760.* Dr. Gotro received a B.S. in mechanical engineering from Marquette University in 1977 and a Ph.D. in materials science from Northwestern University in 1982. In 1986, he was appointed Adjunct Associate Professor of Chemical Engineering and Materials Science at Syracuse University. Since joining IBM in 1982, Dr. Gotro has been studying structure-property-processing relationships in thermosetting polymers. Major efforts have involved the investigation of the chemorheological behavior of thermosetting polymers during lamination along with the evaluation of new materials and processes for multilayer circuit board applications.

Bernd K. Appelt *IBM Systems Technology Division, 1701 North St., Endicott, New York 13760.* Dr. Appelt received his Ph.D. in polymer science in 1977 from the University of Mainz, West Germany. He subsequently spent one year as a Postdoctoral Fellow with Dr. Roger Porter at the University of Massachusetts and one year with Drs. James Lyerla and Augustus Ouano at the IBM Research Laboratory in San Jose, California. In 1980, Dr. Appelt joined the Technology Laboratory in Endicott, New York. He has been active in the area of characterization of thermosets and photoresists, emphasizing thermoanalytical techniques, and is currently manager of a dielectric materials development group.